Am J Physiol Heart Circ Physiol 316: H768–H780, 2019.
First published January 18, 2019; doi:10.1152/ajpheart.00471.2018.

RESEARCH ARTICLE | *Cardiac Excitation and Contraction*

Long-term testosterone deficiency modifies myofilament and calcium-handling proteins and promotes diastolic dysfunction in the aging mouse heart

Omar Ayaz,[1] Shubham Banga,[1] Stefan Heinze-Milne,[1] Robert A. Rose,[3] W. Glen Pyle,[4] and Susan E. Howlett[1,3]

[1]*Department of Pharmacology, Dalhousie University, Halifax, Nova Scotia, Canada;* [2]*Department of Medicine (Geriatric Medicine), Dalhousie University, Halifax, Nova Scotia, Canada;* [3]*Department of Physiology and Pharmacology, Cumming School of Medicine, University of Calgary, Calgary, Alberta, Canada; and* [4]*Department of Biomedical Sciences, University of Guelph, Guelph, Ontario, Canada*

Submitted 13 July 2018; accepted in final form 10 January 2019

Ayaz O, Banga S, Heinze-Milne S, Rose RA, Pyle WG, Howlett SE. Long-term testosterone deficiency modifies myofilament and calcium-handling proteins and promotes diastolic dysfunction in the aging mouse heart. *Am J Physiol Heart Circ Physiol* 316: H768–H780, 2019. First published January 18, 2019; doi:10.1152/ajpheart.00471.2018.—The impact of long-term gonadectomy (GDX) on cardiac contractile function was explored in the setting of aging. Male mice were subjected to bilateral GDX or sham operation (4 wk) and investigated at 16–18 mo of age. Ventricular myocytes were field stimulated (2 Hz, 37°C). Peak Ca^{2+} transients (fura 2) and contractions were similar in GDX and sham-operated mice, although Ca^{2+} transients (50% decay time: 45.2 ± 2.3 vs. 55.6 ± 3.1 ms, $P < 0.05$) and contractions (time constant of relaxation: 39.1 ± 3.2 vs. 69.5 ± 9.3 ms, $P < 0.05$) were prolonged in GDX mice. Action potential duration was increased in myocytes from GDX mice, but this did not account for prolonged responses, as Ca^{2+} transient decay was slow even when cells from GDX mice were voltage clamped with simulated "sham" action potentials. Western blots of proteins involved in Ca^{2+} sequestration and efflux showed that Na^+/Ca^{2+} exchanger and sarco(endo)plasmic reticulum Ca^{2+}-ATPase type 2 protein levels were unaffected, whereas phospholamban was dramatically higher in ventricles from aging GDX mice (0.24 ± 0.02 vs. 0.86 ± 0.13, $P < 0.05$). Myofilament Ca^{2+} sensitivity at physiological Ca^{2+} was similar, but phosphorylation of essential myosin light chain 1 was reduced by ≈50% in ventricles from aging GDX mice. M-mode echocardiography showed no change in systolic function (e.g., ejection fraction). Critically, pulse-wave Doppler echocardiography showed that GDX slowed isovolumic relaxation time (12.9 ± 0.9 vs. 16.9 ± 1.0 ms, $P < 0.05$), indicative of diastolic dysfunction. Thus, dysregulation of intracellular Ca^{2+} and myofilament dysfunction contribute to deficits in contraction in hearts from testosterone-deficient aging mice. This suggests that low testosterone helps promote diastolic dysfunction in the aging heart.

NEW & NOTEWORTHY The influence of long-term gonadectomy on contractile function was examined in aging male hearts. Gonadectomy slowed the decay of Ca^{2+} transients and contractions in ventricular myocytes and slowed isovolumic relaxation time, demonstrating diastolic dysfunction. Underlying mechanisms included Ca^{2+} dysregulation, elevated phospholamban protein levels, and hypophosphorylation of a myofilament protein, essential myosin light chain. Testosterone deficiency led to intracellular Ca^{2+} dysregulation and myofilament dysfunction, which may facilitate diastolic dysfunction in the setting of aging.

aging; excitation-contraction coupling; orchiectomy; sex differences; sex hormones

INTRODUCTION

The rise in the incidence of cardiovascular disease with age, as circulating estrogen and testosterone levels fall, suggests a link between sex steroid hormones and cardiovascular disease (38, 48). Although cardioprotective effects of estrogen have been explored in women (6, 37, 46), the idea that low testosterone contributes to increased cardiovascular risk in aging has only recently received attention (25, 34, 40, 64, 65). Observational studies have shown that low testosterone increases the risk of cardiovascular disease and related mortality in older men (3, 10, 43, 49). This is especially true of diseases characterized by impaired contractility, such as heart failure. Evidence indicates lower testosterone levels in male patients with heart failure (31, 61; but cf. 43) and an increase in heart failure severity as circulating testosterone levels decline (29, 31). Thus, there is an association between low testosterone and impaired cardiac contractility in older men, although the mechanisms involved are not understood.

The biological effects of testosterone are mediated by androgen receptors, which are present in the gonads and in many other tissues, including the heart (15, 16). Importantly, studies in rodent models have shown that androgen receptors are expressed in cardiomyocytes (35, 36). Thus, it is possible that chronic exposure to low testosterone modifies cardiac contractility, at least in part, by effects on the cardiomyocytes themselves. Most studies have inferred information about the effects of testosterone on cardiac contraction in hearts and myocytes isolated from young adult (3−6 mo old) male animals subjected to bilateral gonadectomy (GDX) (for a review, see Ref. 4). Studies in Langendorff-perfused hearts have shown that left ventricular developed pressure is not affected by GDX (9, 47, 57; but cf. 17). The rate of pressure development is also not affected by GDX, but the rate of pressure decay is slowed (17, 47, 50, 52, 57). At the cellular level, most studies have indicated that GDX slows the decay of contractions and Ca^{2+} transients in ventricular myocytes isolated from young male rodents, although whether GDX affects peak responses is

Address for reprint requests and other correspondence: S. E. Howlett, Dept. of Pharmacology, 5850 College St., PO Box 15000, Sir Charles Tupper Medical Bldg., Dalhousie University, Halifax, NS, Canada B3H 4R2 (e-mail: Susan.Howlett@dal.ca).

controversial (9, 13, 27, 45, 47, 54, 57, 60, 62). Less is known about the impact of GDX on cardiac contractile function in vivo, although in vivo studies with M-mode echocardiography have suggested that GDX reduces ejection fraction in young male rats and mice (54, 60). Whether GDX affects diastolic function has not been investigated (54, 60). Together, these findings suggest that low testosterone modifies cardiac contractile function, at least in young adult animals.

Although testosterone deficiency affects contractile function in hearts from young animals, most cardiovascular disease occurs in older individuals (38, 48). Growing evidence suggests that the heart undergoes distinct cellular, structural, and functional changes as a consequence of normal aging, which may adversely affect contractile function (19, 22, 26, 33). Our group has shown that cardiac contractile function declines with age at the organ and cellular levels in male mice (23, 28, 30). This may increase the risk of heart failure with reduced ejection fraction in the setting of aging. We have also shown that relaxation rates and Ca^{2+} transient decay rates are prolonged in aging male mice (23, 28, 30). This may promote diastolic dysfunction as well as heart failure with preserved ejection fraction (HFpEF), which is common in older individuals (58).

It is possible that the effects of age on cardiac contractile function are exacerbated by chronic exposure to low testosterone, although this has not been established. This is important, because it could provide a mechanistic explanation for links between low testosterone levels and heart failure in the aging population. The goal of the present study was to investigate the impact of long-term testosterone deficiency on cardiac contractile function in the setting of aging. In vivo, cellular, and molecular experiments were conducted in aging (16−18 mo old) male C57BL/6 mice subjected to GDX or sham operation at a young age to determine whether long-term testosterone deficiency exacerbates adverse effects of aging on cardiac contractile function.

MATERIALS AND METHODS

Animals. All animal protocols were approved by the Dalhousie University Committee on Laboratory Animals and conformed with the *Guide to the Care and Use of Experimental Animals* (Canadian Council on Animal Care, Ottawa, ON, Canada, vol. 1, 2nd ed., 1993, and vol. 2, 1984). Male C57BL/6J mice were obtained from Charles River Laboratories (St. Constant, QC, Canada). Mice were subjected to bilateral removal of the testes (GDX) or a similar surgery that left the testes intact (sham) at 1 mo of age. Mice were used in experiments at 16–18 mo of age. In some experiments, 5- to 6-mo-old sham and GDX mice also were used to investigate the impact of age and GDX on serum testosterone levels. In each mouse, GDX was confirmed visually by the absence of testes. Mice were housed at the Carleton Animal Care Facility at Dalhousie University and maintained on a 12:12-h light-dark cycle with free access to food and water.

Cell experiments. Ventricular myocytes were isolated by enzymatic dissociation and used in field stimulation, current-clamp, and voltage-clamp experiments with our established techniques (20, 21, 55). Briefly, mice were weighed and anesthetized (200 mg/kg ip pentobarbital sodium with 100 units heparin). The aorta was cannulated to perfuse the heart (2 ml/min, 10 min) with Ca^{2+}-free buffer containing (in mM) 105 NaCl, 5 KCl, 25 HEPES, 0.33 NaH_2PO_4, 1.0 $MgCl_2$, 20 glucose, 3.0 Na-pyruvate, and 1.0 lactic acid (pH 7.4, 37°C, gassed with 100% O_2). The heart was perfused with this buffer plus 50 μM Ca^{2+}, collagenase type 1 (8 mg/30 ml, 250 U/mg, Worthington), dispase II (3.5 mg/30 ml, Roche), and trypsin (0.5 mg/30 ml, Sigma). After 8–10 min, the ventricles were excised, minced, and stored in a high-K^+ buffer containing (in mM) 50 L-glutamic acid, 30 KCl, 30 KH_2PO_4, 20 taurine, 10 HEPES, 10 glucose, 3 $MgSO_4$, and 0.5 EGTA (pH 7.4, room temperature). Cells were filtered with a 225-μm polyethylene mesh filter (Spectra/Mesh).

Cells were loaded with Ca^{2+}-sensitive dye (fura 2-AM, 2.5 μM; Invitrogen, Burlington, ON, Canada) for 20 min in darkness in a chamber on an inverted microscope (Nikon Eclipse TE200, Nikon Canada, Mississauga, ON, Canada). In all experiments, cells were superfused (3 ml/min) with standard buffer (mM): 145 NaCl, 10 glucose, 10 HEPES, 4 KCl, 1 $CaCl_2$, and 1 $MgCl_2$ (pH 7.4, 37°C). For simultaneous recording of cell shortening and Ca^{2+} transients, a custom-made dichroic mirror (Chroma Tech, Rockingham, VT) was used to split the microscope light between a camera (model TM-640, Pulnix America) and a photomultiplier tube (PTI, Brunswick, NJ). Cells were imaged on a closed-circuit television monitor connected to a video edge detector (Crescent Electronics, Sandy, UT) that measured cell length (120 samples/s). A DeltaRAM fluorescence system (Photon Technologies, Birmingham, NJ) was used to excite cardiomyocytes at 340 and 380 nm. Felix software (Photon Technologies) was used to record fluorescence emission (at 510 nm) for both wavelengths (200 samples/s). Background fluorescence was subtracted from all recordings, and the ratio of emissions was used for conversion to intracellular Ca^{2+} concentrations via an in vitro calibration curve, as previously described (20, 55).

For field stimulation experiments, cells were paced at 2 Hz with bipolar pulses via platinum electrodes coupled to a stimulus isolation unit (model SIU-102, Warner Instruments, Hamden, CT) controlled by pClamp 8.1 software (Molecular Devices, Sunnyvale, CA). In some experiments, the pacing frequency was increased to 4 Hz. Stimulation was stopped after 30 s, but recording continued for an additional 10 s to allow detection of spontaneous contractions, if present. Current- and voltage-clamp recordings were made with high-resistance (18−25 MΩ) microelectrodes (filled with filtered 2.7 M KCl) and an Axoclamp 2B amplifier controlled by pClamp software (Molecular Devices). Current-clamp mode was used to record action potentials; cells were paced with 3-ms pulses delivered at a frequency of 2 Hz to match the field stimulation protocol. For voltage-clamp experiments, we used high-resistance microelectrodes and discontinuous single-electrode voltage-clamp techniques (switch clamp, 5–8 kHz) with established techniques used in our previous studies (20, 21, 23, 28, 41, 42). The use of high-resistance microelectrodes plus switch clamp allows us to voltage clamp cells with minimal dialysis of the intracellular milieu to avoid buffering internal Ca^{2+}. In these experiments, simulated "sham" and "GDX" action potential waveforms were created from mean values recorded from myocytes from sham and GDX mice, as described below in RESULTS. Myocytes from sham and GDX mice were then voltage clamped with trains (2 Hz) of these simulated action potentials, characteristic of cells from sham or GDX mice, and Ca^{2+} transients were recorded simultaneously.

Western blots for Ca^{2+}-handling proteins. Western blot analysis was used to compare the levels of major Ca^{2+}-handling proteins in ventricles from aging sham and GDX mice. Mice were anesthetized as described above, and hearts were removed. The ventricles were weighed, flash frozen in liquid nitrogen, and stored at −80°C until use. Tibia length was also measured and used as an index of heart weight. The ventricles were homogenized (1 min) with a glass Dounce homogenizer (Sigma) in cold RIPA buffer containing 1% Triton X-100, 1% sodium deoxycholate, 0.1% SDS, 150 mM NaCl, 50 mM Tris·HCl (pH 7.8), 1 mM EDTA, and 1 mM EGTA plus a protease inhibitor cocktail (Halt protease inhibitor cocktail, Thermo Scientific) and a phosphatase inhibitor cocktail (Halt phosphatase inhibitor cocktail, Thermo Scientific). The homogenate was centrifuged (12,000 rpm, 4°C, Beckman Coulter) for 10 min, and the supernatant was divided into aliquots and stored at −80°C. The protein concentration for each sample was quantified with a DC protein assay (Bio-Rad).

Table 1. *Physical characteristics and morphometric data for sham and GDX mice*

Parameter	Sham	GDX	*P* Value
Body weight, g	45.5 ± 3.4 (9)	43.3 ± 3.0 (9)	0.63
Heart weight, mg	241.4 ± 19.6 (9)	200.2 ± 12.9 (9)	0.10
Heart weight/body weight, mg/g	5.4 ± 0.4 (9)	4.7 ± 0.3 (9)	0.17
Heart weight/tibia length, mg/mm	11.2 ± 0.9 (5)	9.6 ± 1.0 (5)	0.28
Cell length, μm	131.2 ± 3.7 (49)	123.5 ± 3.8 (41)	0.16
Cell width, μm	28.5 ± 1.1 (49)	26.1 ± 1.2 (41)	0.14
Cell area, μm^2	3,737.6 ± 185.9 (49)	3,266.3 ± 206.8 (41)	0.045*
Cell length-to-width ratio	5.0 ± 0.2 (49)	5.1 ± 0.3 (41)	0.63
Wet lung weight, g	0.17 ± 0.01 (3)	0.17 ± 0.01 (3)	0.84
Lung wet weight-to-dry weight ratio	4.08 ± 0.20 (3)	4.24 ± 0.48 (3)	0.78

Values are means ± SE; sample sizes are shown in parentheses. GDX, gonadectomized. *$P < 0.05$.

Homogenates were reconstituted in 4× Laemmli sample buffer and heated (95°C, 5 min). Equal amounts of sham and GDX sample protein (25 μg/well) were resolved on 7% polyacrylamide gels in all Western blot experiments. The primary antibodies were Na^+/Ca^{2+} exchanger (NCX; 1:1,000 dilution, catalog no. R3F1, Swant), sarco-(endo)plasmic reticulum Ca^{2+}-ATPase type 2 (SERCA2; 1:2,000 dilution, catalog no. MA3-919, ThermoFisher Scientific), phospholamban (PLB; 1:5,000 dilution, catalog no. A010-12, Badrilla), and β-actin (1:10,000 dilution, catalog no. A5441, Sigma). The secondary antibodies were anti-mouse (1:20,000 dilution, catalog no. ab97046, Abcam) and anti-rabbit (1:20,000 dilution, catalog no. ab6721, Abcam) horseradish peroxidase-conjugated polyclonal antibodies. The membrane was incubated for 5 min with Clarity Western ECL substrate (Bio-Rad), and protein chemiluminescence signals were imaged using a ChemiDoc MP system (Bio-Rad Laboratories, Mississauga, ON, Canada). Protein band intensities were quantified with ImageJ software (v1.34, National Institutes of Health). Target proteins were normalized to β-actin or by staining the polyvinylidene difluoride membrane with amido black (naphthol blue, Sigma) to verify equal protein loading.

Myofilament experiments. Myofilaments were isolated using techniques we have previously described (24). The protocol for harvesting the ventricles is described above (see *Western blots for Ca^{2+}-handling proteins*). The tissue was homogenized in ice-cold buffer containing (in mM) 60 KCl, 30 imidazole (pH 7.0), 2 $MgCl_2$, 0.01 leupeptin, 0.1 PMSF, 0.2 benzamidine, and phosphatase inhibitors (catalog no. P0044, Sigma-Aldrich). The homogenate was centrifuged (14,000 *g*, 15 min, 4°C), and the pellet was resuspended in the buffer described above for tissue homogenization plus 1% Triton X-100 for 45 min on ice. This solution was centrifuged (1,100 *g*, 15 min, 4°C), and the pellet containing the myofilaments was washed three times in ice-cold buffer and then resuspended in homogenization buffer. The myofilaments were either flash frozen to assess myofilament protein phosphorylation or kept on ice and used immediately to evaluate actomyosin Mg^{2+}-ATPase activity. Actomyosin Mg^{2+}-ATPase activity was measured by incubation of the myofilaments (25 μg) in ATPase buffers that contained variable concentrations of free Ca^{2+} (10 min, 32°C) using techniques we have previously described (63). The reaction was quenched by the addition of 10% trichloroacetic acid. Equal volumes of $FeSO_4$ (0.5%) and ammonium molybdate (0.5%) in 0.5 M H_2SO_4 were added, and absorbance at 630 nm was read to quantify production of inorganic phosphate.

Phosphorylation of major myofilament proteins was investigated as we have previously described (24). Myofilament proteins (10 μg) were separated by SDS-PAGE (12%) and then fixed in 50% methanol-10% acetic acid (23°C) overnight. Myofilament protein phosphorylation was assessed with Pro-Q Diamond staining according to the manufacturer's instructions (Molecular Probes, Eugene, OR). The gels were imaged with a ChemiDoc MP imaging system (Bio-Rad Laboratories) and analyzed with ImageJ software. The gels were stained with Coomassie blue dye for the determination of protein loading, and actin was used as a loading control.

Echocardiography. Mice were anesthetized with 2% isoflurane in oxygen and placed in the supine position on a 37°C platform, and ECG was monitored with subcutaneous limb electrodes. Two-dimensional, guided M-mode echocardiography was then performed with a high-resolution linear transducer (model i13L, GE Ultrasound, Horten, Norway) and a Vivid 7 imaging system (GE Medical Systems, Horten, Norway). Images were generated in M-mode, and ECG recordings were used to determine heart rate. Systolic and diastolic ventricular dimensions were measured to determine or derive the following parameters: interventricular septum thickness at diastole and end systole, left ventricular internal diameter at diastole and end systole, left ventricular posterior wall thickness at diastole and end systole, relative wall thickness, left ventricular mass, fractional shortening, ejection fraction, and stroke volume. Diastolic function was evaluated with pulse-wave Doppler echocardiography in the apical long-axis view. Maximal transmitral inflow velocities were recorded by setting the sample volume near the tip of the mitral leaflets in the mitral orifice, parallel to the direction of blood flow. From the pulse-wave Doppler waveforms, we assessed the following parameters: peak early transmitral velocity (E wave) and peak late transmitral velocity (A wave), *E*-to-*A* ratios, E wave deceleration time, and isovolumic relaxation time.

Serum testosterone analysis. A mouse ELISA kit (Crystal Chem, Elk Grove Village, IL) was used to compare serum testosterone levels in adult and aged sham and GDX mice. Blood was obtained from the facial vein in anesthetized mice. Serum was isolated using a standard protocol. Briefly, the blood was left for 30 min at room temperature and then processed for 10 min using an Eppendorf centrifuge (1,500 *g*, 4°C). The supernatant (serum) was stored at −20°C until use. The testosterone assay was performed following the manufacturer's instructions. Serum was thawed on ice, and 10-μl standards and samples were transferred via pipette onto the 96-well ELISA plate. The plate

Table 2. *Serum testosterone levels in adult and aged sham and GDX mice*

	Testosterone, ng/ml	Sample Size
Adult		
Sham	1.15 ± 0.43	9
GDX	0.01 ± 0.01*	10
Aged		
Sham	0.86 ± 0.41	7
GDX	0.05 ± 0.02*	8

Values are means ± SE. GDX, gonadectomized. *$P < 0.05$ (by two-way ANOVA).

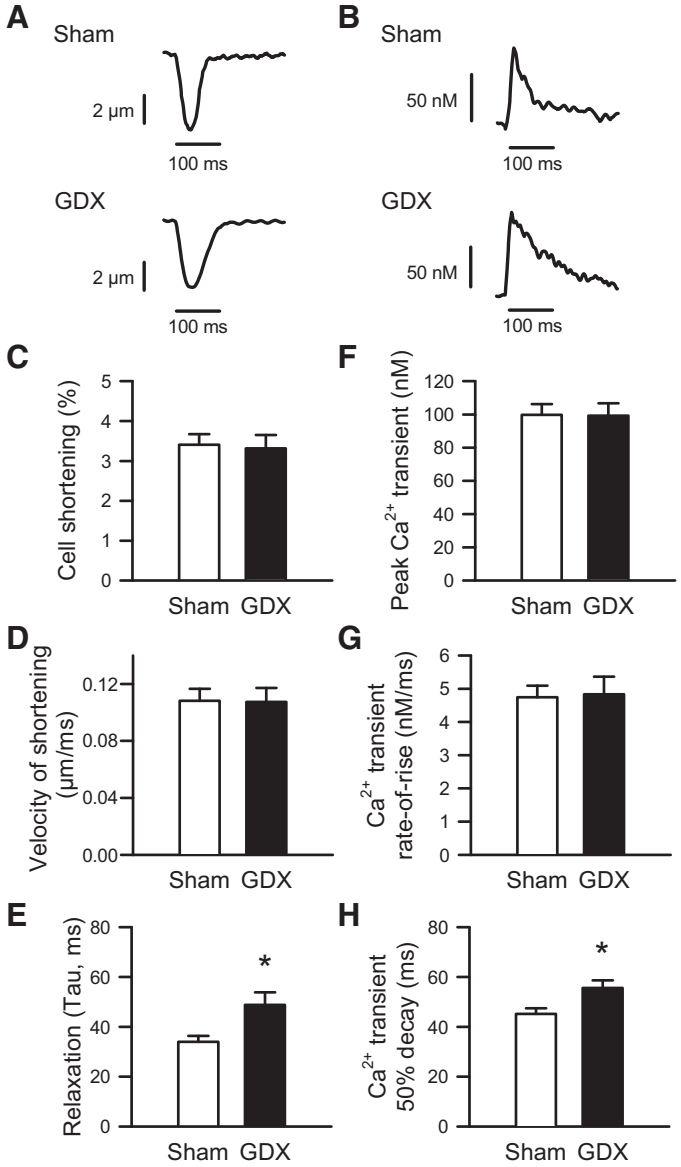

Fig. 1. Long-term testosterone deficiency prolonged relaxation and Ca^{2+} transient decay in isolated ventricular myocytes. Myocytes were loaded with fura 2-AM and field stimulated at 2 Hz, and contractions and Ca^{2+} transients were recorded simultaneously. *A* and *B*: representative traces of contractions (*left*) and Ca^{2+} transients (*right*) in myocytes from sham-operated (sham) and gonadectomized (GDX) mice. Responses appeared similar in size, with slower decay in the GDX cell than sham control cell. *C*: peak contractions normalized to resting cell length (cell shortening) were similar in sham and GDX groups. *D*: velocity of shortening did not differ between GDX and sham control groups. *E*: time course of cell lengthening (τ) was prolonged in the GDX group compared with the sham control group. *F* and *G*: peak Ca^{2+} transient amplitudes and rates of rise were similar in GDX and sham control groups. *H*: time to 50% decay of the Ca^{2+} transient was significantly increased in GDX mice compared with sham control mice. Values are means ± SE; $n = 49$ sham and 41 GDX cells isolated from 8 sham and 7 GDX mice. *$P < 0.05$ (by *t*-test).

was activated by addition of the enzyme conjugate plus incubation buffer and then incubated with shaking at 600 rpm at room temperature (1 h). The plate was washed four times with buffer, the substrate was added, and the plate was incubated in darkness for 30 min at room temperature. The reaction was stopped, and absorbance at 450- and 630-nm wavelengths was measured using a Fluostar Omega microplate reader. Serum testosterone concentrations were calculated from a four-parameter logistic curve fit, as recommended.

Data analyses. Field stimulation and electrophysiology data were analyzed using Clampfit 8.2 (Molecular Devices). In field stimulation experiments, 50 contractions or Ca^{2+} transients were averaged, and responses were then measured. Peak cell shortening was measured as the difference between cell length at rest and the peak contraction. The velocity of cell shortening was measured to quantify the rate of shortening. The relaxation phase was fit with an exponential function to measure the time constant of relaxation (τ). Peak Ca^{2+} transients were measured as the difference between diastolic and systolic Ca^{2+} levels. The rate of rise of Ca^{2+} transients and the time to 50% decay were also measured. Sigmaplot (version 12.5, Systat Software) was used for all statistical analyses and curve-fitting analyses as well as figure construction. Values are means ± SE. Differences between means were tested using a Student's *t*-test. A nonparametric Mann-Whitney rank sum test was used for data that were not normally distributed. Differences were considered significant if $P < 0.05$.

Chemicals. All chemicals, unless otherwise stated, were purchased from Sigma-Aldrich (Oakville, ON, Canada) or BDH (Toronto, ON, Canada). Fura 2-AM was prepared in anhydrous DMSO and stored at −20°C.

RESULTS

Physical characteristics, morphometric data, and serum testosterone levels for sham and GDX male mice. We first compared physical characteristics of aging sham and GDX mice and their hearts. Both groups of mice were similar in body weight (Table 1). Heart weights were lower in GDX than sham animals, but this difference was not statistically signifi-

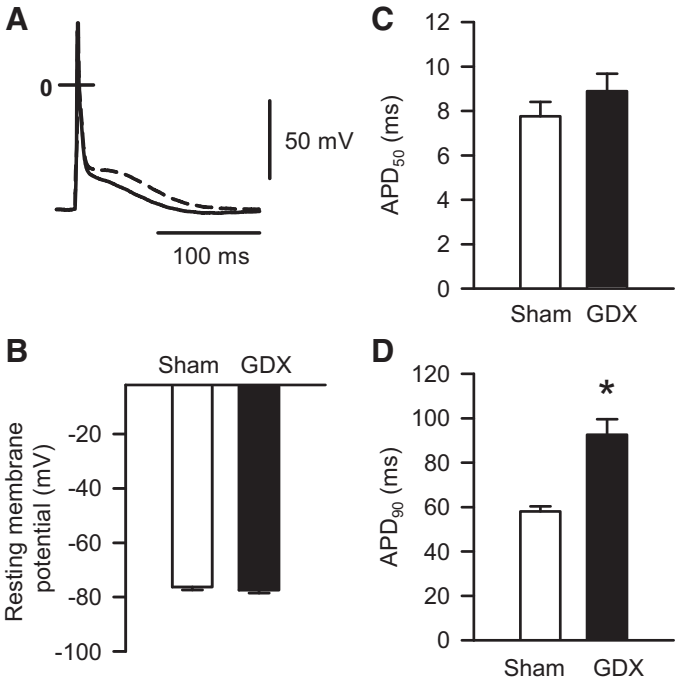

Fig. 2. Chronic testosterone deficiency prolonged action potential duration (APD) in isolated ventricular myocytes. *A*: representative action potentials recorded in myocytes from sham-operated (sham; solid trace) and gonadectomized (GDX; dashed trace) mice stimulated at 2 Hz. *B*: mean resting membrane potentials were similar in sham and GDX groups. *C*: APD at 50% repolarization (APD_{50}) was not affected by GDX. *D*: APD at 90% repolarization (APD_{90}) was prolonged in GDX mice compared with sham control mice. Values are means ± SE; $n = 9$ sham and 12 GDX myocytes isolated from 3 sham and 3 GDX mice. *$P < 0.05$ (by *t*-test).

cant, even when heart weights were normalized to either body weight or tibia length (Table 1). Although cell lengths and widths were similar in the two groups, myocyte cross-sectional area was significantly smaller in GDX than sham control mice (Table 1). There was no significant difference in length-to-width ratios between groups (Table 1), which suggests a proportional reduction in size in GDX cells. Together, these data suggest that long-term testosterone deficiency in older animals causes a small, but significant, decrease in ventricular myocyte size compared with sham control animals. Wet lung weight and the ratio of wet lung weight to dry lung weight were quantified as an index of pulmonary congestion/heart failure (1). There was no significant difference in lung weight between sham and GDX mice (Table 1). Table 2 shows serum testosterone levels for adult (5−6 mo old) and aged (≈18 mo old) sham and GDX mice. These data show no significant decline in circulating testosterone levels with age but a marked decrease after GDX in both age groups.

Impact of GDX on contractions, Ca^{2+} transients, and action potential configuration in ventricular myocytes from aging mice. The next series of experiments investigated whether long-term GDX modified contractions and Ca^{2+} transients in the setting of aging. Cells were field stimulated at 2 Hz, and cell shortening and Ca^{2+} transients were recorded simultaneously. Representative examples from a sham myocyte and a GDX myocyte are shown in Fig. 1, *A* and *B*. Mean data clearly demonstrated that peak contraction (Fig. 1*C*) and the velocity of shortening (Fig. 1*D*) were similar in the two groups, but the rate of relaxation was prolonged in cells from aging GDX mice (Fig. 1*E*). Parallel changes occurred in the underlying Ca^{2+} transients. Although peak Ca^{2+} transients (Fig. 1*F*) and their rates of rise (Fig. 1*G*) were not affected, the time to 50% decay was significantly prolonged in cells from GDX animals (Fig. 1*H*). In some experiments, pacing frequency was increased to 4 Hz, which is closer to the physiological heart rate for mice. We found that the mean Ca^{2+} transient time to 50% decay at 4 Hz was also prolonged by GDX (38.8 ± 1.5 and 44.8 ± 1.8 ms for sham and GDX groups, respectively, $P = 0.01$). The number of spontaneous contractions after the stimulus was stopped was significantly higher in myocytes from GDX than sham control mice (1.5 ± 0.5 vs. 4.9 ± 1.6, $P = 0.02$). Thus, long-term GDX caused a marked prolongation of the decay rates of myocyte contractions and Ca^{2+} transients as well as an increase in spontaneous beats. These findings indicate dysregulated intracellular Ca^{2+} homeostasis in hearts from aging, testosterone-deficient mice.

When myocytes are field stimulated, responses are activated by action potentials. A difference in action potential configuration between cardiomyocytes from sham and GDX mice may help prolong contractions and Ca^{2+} transients in cells from GDX mice. To test this idea, action potentials were recorded in sham and GDX cells in current-clamp mode (Fig. 2). Representative examples of action potentials recorded from the two groups are shown in Fig. 2*A*. Mean data demonstrated no significant difference in either resting membrane potential (Fig. 2*B*) or action potential duration (APD) at 50% repolarization (APD_{50}; Fig. 2*C*). On the other hand, GDX was associated with a significant increase in APD at 90% repolarization (APD_{90}) in myocytes from aging hearts (Fig. 2*D*). This increase in APD would be expected to prolong the duration of depolarization and could account for the longer Ca^{2+} transients in myocytes from GDX mice. To investigate this, simulated sham and GDX action potential waveforms were created based on mean action potential configurations (Fig. 3, *A* and *C*). Cells from sham and GDX mice were then voltage clamped with trains of simulated sham (short) and GDX (longer) action potentials delivered at a frequency of 2 Hz as in the field stimulation experiments. Ca^{2+} transient decay rates remained prolonged in GDX cells com-

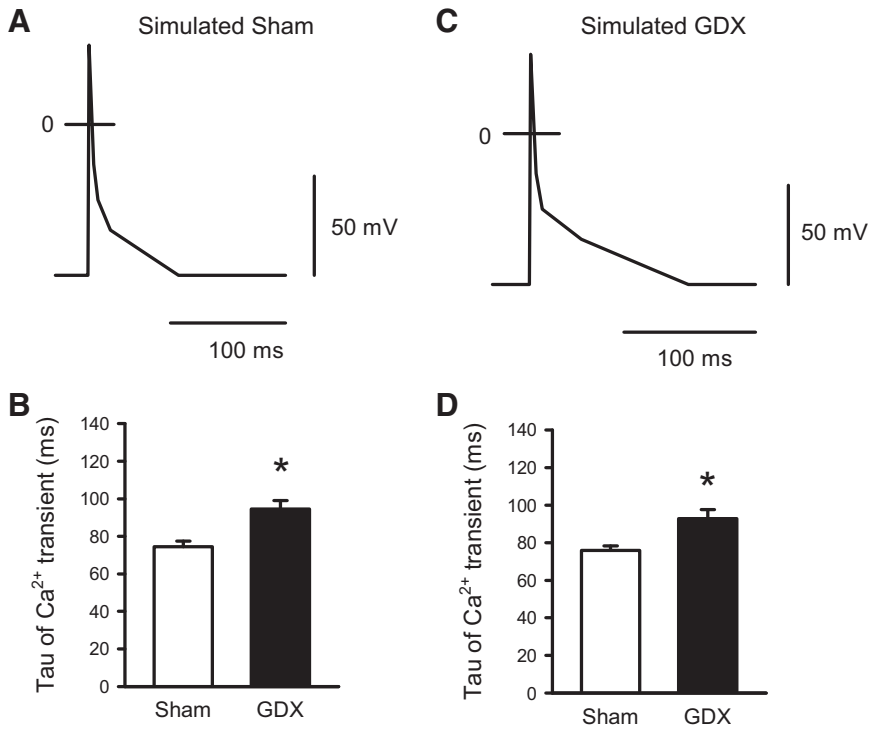

Fig. 3. Ca^{2+} transients were prolonged in myocytes from gonadectomized (GDX) mice when cells were voltage clamped with simulated "sham" and "GDX" action potential waveforms. Cells were loaded with fura 2-AM, voltage clamped with simulated action potential waveforms, and paced at 2 Hz, and Ca^{2+} transients were recorded. *A*: a simulated sham action potential based on the average action potential configuration recorded in myocytes from sham mice. *B*: Ca^{2+} transients were longer for GDX than sham control mice when myocytes were paced with the shorter action potentials characteristic of cells from the sham control group. *C*: a simulated GDX action potential was created from the average action potential configuration recorded in cells from GDX mice. *D*: Ca^{2+} transients were prolonged in cells from GDX mice when they were paced with the longer GDX action potential. τ, Time course of cell lengthening. Values are means ± SE; $n = 4$ sham and 6 GDX myocytes isolated from 2 sham and 2 GDX mice. *$P <$ 0.05 (by *t*-test).

pared with sham cells, regardless of APD (Fig. 3, *B* and *D*). These findings indicate that although APD is prolonged in aging myocytes from GDX compared with sham control mice, this does not account for the slower Ca^{2+} transient decay observed in GDX cells.

Western blots of proteins involved in Ca^{2+} efflux and sequestration in ventricles from aging sham and GDX mice. To explore mechanisms involved in Ca^{2+} dysregulation, we used Western blot analysis to compare the levels of major proteins involved in Ca^{2+} efflux and Ca^{2+} sequestration in the ventricles of aging sham and GDX mice. Our results showed that levels of NCX protein, which functions primarily to remove Ca^{2+} from the myocyte, were virtually identical in the two groups (Fig. 4*A*). Thus, slower Ca^{2+} transients in GDX cells were not due to reduced Ca^{2+} efflux through NCX. We also showed that SERCA2 protein levels were similar in ventricles from aging sham-operated and GDX mice (Fig. 4*B*). This demonstrates that the slower Ca^{2+} transient decay rates in myocytes from GDX mice were not explained by a decrease in protein levels of this important sarcoplasmic reticulum Ca^{2+} sequestration mechanism. We also compared PLB protein levels in hearts from sham and GDX mice and showed that PLB protein levels were dramatically higher in aging GDX than sham control hearts (Fig. 4*C*). This observation suggests that the prolonged Ca^{2+} transient decay in myocytes from aging GDX mice is attributable, at least in part, to an increase in PLB.

Impact of GDX on myofilament Ca^{2+} sensitivity and myofilament protein phosphorylation in the aging heart. Long-term GDX may also affect cardiac contraction at the myofilament level. To determine if GDX modified myofilament Ca^{2+} sensitivity, actomyosin Mg^{2+}-ATPase activity was measured in ventricles from aging sham and GDX mice. Figure 5*A* shows actomyosin Mg^{2+}-ATPase activity expressed as a function of Ca^{2+} concentration for ventricles from sham and GDX mice. The curves were not statistically different except that maximal actomyosin Mg^{2+}-ATPase activity was higher in hearts from GDX mice. However, this was only seen at the highest, supraphysiological, Ca^{2+} concentration. When the data were normalized to the maximal activity for each group, curves for sham and GDX groups overlapped (Fig. 5*B*), which suggests that there was no difference in normalized actomyosin Mg^{2+}-ATPase activity. This was quantified by comparing the concentration of Ca^{2+} required to produce a 50% increase in activity (EC_{50} values), which was similar in the two groups (Fig. 5*C*). Hill coefficients also were not affected by GDX (Fig. 5*D*). These results suggest that changes in myofilament Ca^{2+} sensitivity are unlikely to contribute to the contractile dysfunction in hearts from GDX mice.

Because phosphorylation strongly influences myofilament function, phosphorylation levels of critical myofilament proteins were compared in the two groups (Fig. 6). Myofilament proteins were stained with Pro-Q Diamond to compare phosphorylation of myofilament proteins in hearts from sham and GDX mice (Fig. 6*A*, *left*). The gels were then stained with Coomassie blue dye to examine total protein load (Fig. 6*A*, *right*). GDX did not affect phosphorylation of most major myofilament proteins, including myosin-binding protein C, desmin, troponin T, tropomyosin, troponin I, and regulatory myosin light chain/myosin light chain 2 (Fig. 6*B*). In contrast,

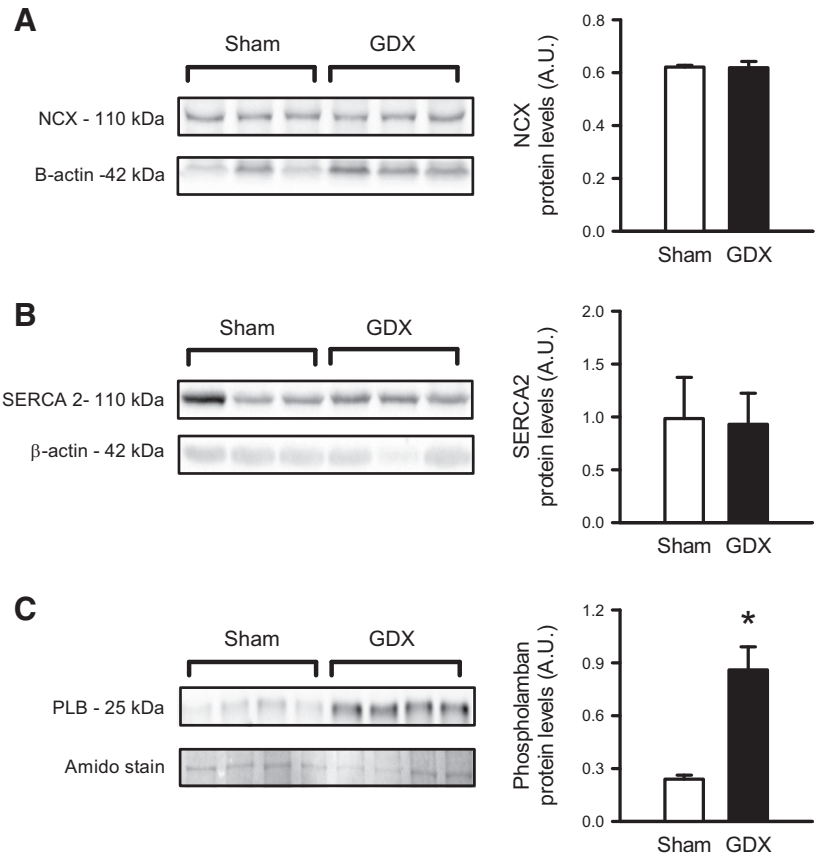

Fig. 4. Gonadectomy (GDX) increased levels of phospholamban (PLB) protein in ventricles from aging mice but had no effect on Na^+/Ca^{2+} exchanger (NCX) or sarco(endo)plasmic reticulum Ca^{2+}-ATPase (SERCA) protein levels. *Left*: representative Western blots illustrate major Ca^{2+}-handling proteins (*top*) and loading controls (*bottom*) in aging hearts from sham-operated (sham) and GDX mice. *Right*: mean normalized protein. *A*: NCX protein levels were similar in ventricles from sham and GDX mice. *B*: SERCA2 protein levels were similar in hearts from aging sham and GDX mice. *C*: PLB protein levels were significantly higher in hearts from aging GDX than sham mice. AU, arbitrary units. Values are means ± SE; $n = 3$ sham and 3 GDX hearts (*A* and *B*) and 4 sham and 4 GDX hearts (*C*). $^*P < 0.05$ (by *t*-test).

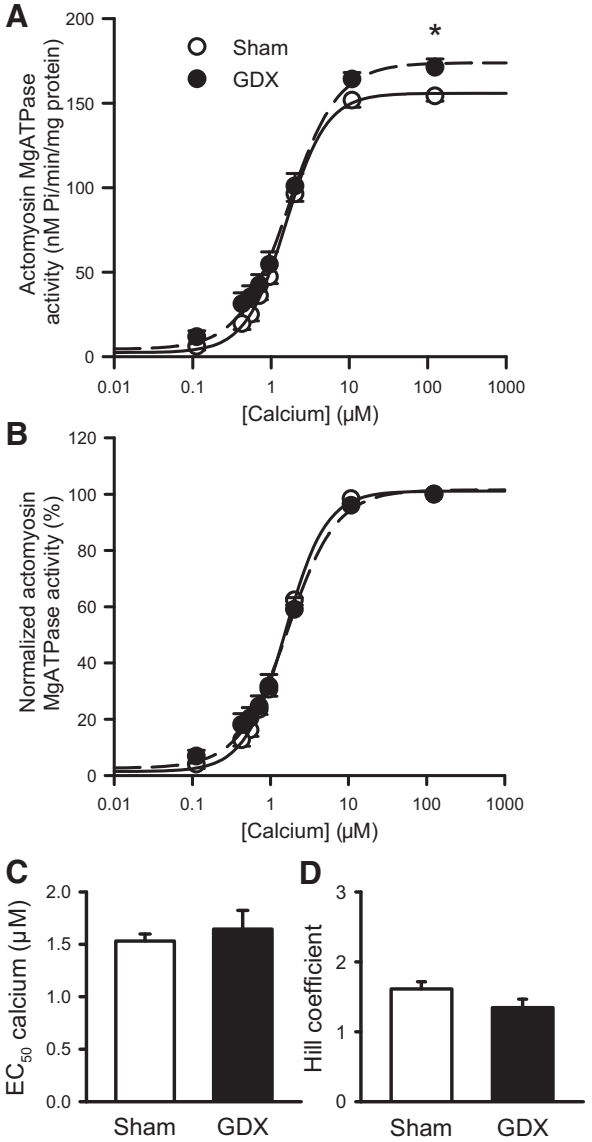

Fig. 5. Myofilament Ca^{2+} sensitivity was similar in aging hearts from sham-operated (sham) and gonadectomized (GDX) mice, although maximal ATPase activity was higher at saturating Ca^{2+} concentrations in hearts from GDX mice. Myofilament Ca^{2+} sensitivity in the ventricles was assayed as actomyosin Mg^{2+}-ATPase activity. *A*: long-term GDX increased maximum actomyosin ATPase activity compared with the sham control group. *B*: myofilament Ca^{2+} sensitivity was similar in sham and GDX mice when actomyosin Mg^{2+}-ATPase activity was normalized to maximal activity in each group. *C*: EC_{50} values were similar in hearts from sham and GDX mice. *D*: Hill coefficients did not differ between sham and GDX samples. Values are means ± SE; $n = 4$ sham and 5 GDX hearts. *$P < 0.05$ (by *t*-test).

there was a marked decrease in phosphorylation of essential myosin light chain/myosin light chain 1 (ELC), one of two regulatory myosin light chains, in hearts from GDX compared with sham control mice (Fig. 6*B*). Thus, long-term GDX is associated with a marked decrease in phosphorylation of a key myosin regulatory protein in the aging heart.

Influence of long-term GDX on myocardial systolic and diastolic function in vivo in the setting of aging. Inasmuch as GDX slows cardiac relaxation at the cellular level, it would be expected to slow cardiac contraction in vivo. To test this, we used echocardiography to compare systolic and diastolic function in sham and GDX mice. Figure 7, *A* and *B*, shows representative M-mode recordings used to evaluate cardiac structure and systolic function in the two groups. Representative pulse-wave Doppler recordings used to evaluate diastolic function in sham and GDX mice are shown in Fig. 7, *C* and *D*. Data for key echocardiography measurements are shown in Fig. 8; additional data are shown in Table 3. In terms of functional parameters, there was no effect of GDX on heart rate, ejection fraction, or fractional shortening (Fig. 8, *A*–*C*). We also evaluated structural parameters and found that GDX had no effect on left ventricular internal diameter and left ventricular posterior wall thickness at systole or diastole (Fig. 8, *D* and *E*, and Table 3). In contrast, long-term GDX was associated with a thinning of the interventricular septum at systole and diastole (Fig. 8*F* and Table 3) and with a significant decrease in left ventricular mass in the aging heart (Fig. 8*G*). We also assessed diastolic function with pulse-wave Doppler echocardiography and found that although GDX had no effect on E-wave deceleration time (Fig. 8*H*) or *E*-to-*A* ratio (Fig. 8*I*), it did cause a marked prolongation of isovolumic relaxation time (Fig. 8*J*). Together, these findings suggest that long-term GDX reduces left ventricular mass, promotes septal thinning, and slows myocardial relaxation in vivo in the setting of aging.

DISCUSSION

The objective of the present study was to investigate the impact of long-term GDX on cardiac contractile function in the setting of aging. We found that ventricular myocytes were smaller and rates of decay for contractions and Ca^{2+} transients were slower in GDX mice than in sham control mice. APD also was prolonged in myocytes from aging GDX compared with sham control mice, but this did not account for the slower Ca^{2+} transients. Indeed, Ca^{2+} transient decay was slow in the GDX group, even when cells were voltage clamped with simulated sham action potentials. To investigate underlying mechanisms, we compared proteins involved in Ca^{2+} sequestration and efflux in hearts from aging sham and GDX mice. Although NCX and SERCA2 protein levels were unaffected by GDX, PLB protein was dramatically higher in hearts from aging GDX mice than control mice. Higher levels of PLB could prolong Ca^{2+} uptake into the sarcoplasmic reticulum and help explain prolonged Ca^{2+} transient decay in myocytes from aging GDX mice. Although myofilament Ca^{2+} sensitivity was similar in the two groups, phosphorylation of the regulatory myosin light chain ELC was reduced in hearts from aging GDX mice. Thus, changes in myofilaments in hearts from GDX mice also may contribute to changes in contractile function. Long-term GDX was also associated with structural and functional changes in the aging heart in vivo, where GDX reduced left ventricular mass and promoted septal thinning. Critically, GDX also slowed isovolumic relaxation time, which suggests that chronic exposure to low testosterone may promote diastolic dysfunction in the aging heart.

Previous work in ventricular myocytes from young adult male rodents showed that GDX resulted in smaller, slower contractions and Ca^{2+} transients (9, 13, 27, 45, 47, 54, 57, 60, 62). In contrast, we found that long-term GDX had no effect on peak responses in ventricular myocytes from aging animals but prolonged contractions and the underlying Ca^{2+} transients. This was seen even when we increased the pacing frequency to

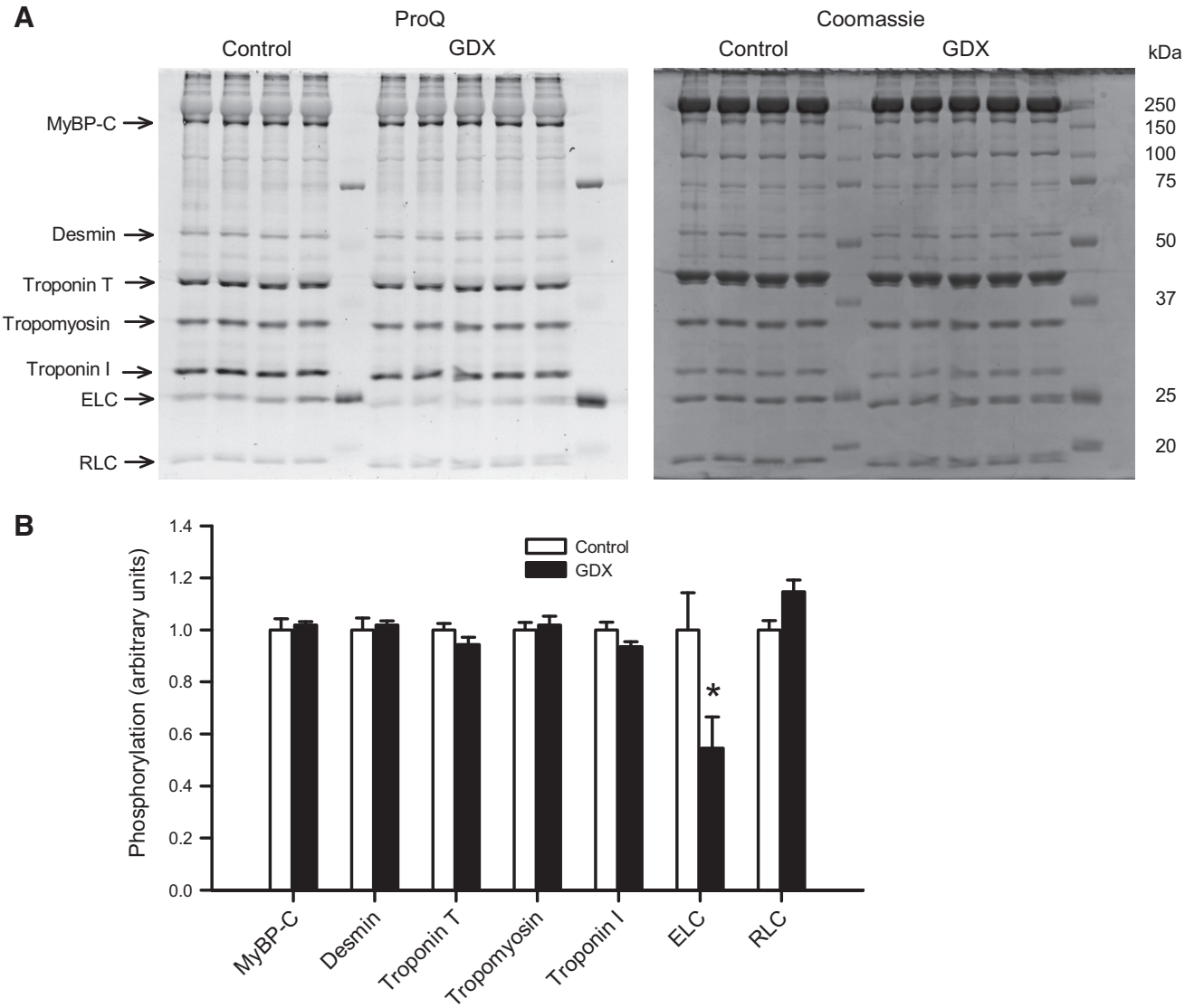

Fig. 6. Myofilament protein phosphorylation in ventricles from aging sham-operated (sham) and gonadectomized (GDX) mice. *A*: myofilament proteins were separated by SDS-PAGE and then stained with Pro-Q Diamond (*left*) to compare phosphorylation of myofilament proteins in hearts from sham and GDX mice. Gels were subsequently stained with Coomassie blue dye (*right*) to determine total protein load. Approximate molecular weights of myofilament proteins are also shown. *B*: phosphorylation of essential myosin light chain/myosin light chain 1 (ELC) was significantly lower in ventricles from mice subjected to long-term GDX than in sham control mice. There were no other statistically significant differences in phosphorylation status between sham and GDX mice. MyBP-C, myosin-binding protein C; RLC, regulatory myosin light chain/myosin light chain 2. Values are means ± SE; $n = 4$ sham and 5 GDX hearts. *$P < 0.05$ (by *t*-test).

4 Hz, which is closer to the physiological rate for mice (2). These observations strongly suggest that the combination of testosterone deficiency and advanced age leads to marked slowing of relaxation in myocytes from the aging heart. Unlike previous studies where contractions or Ca^{2+} transients were recorded separately (9, 13, 27, 45, 47, 54, 57, 60, 62), we recorded responses simultaneously. Thus, our data directly demonstrate that dysregulation of intracellular Ca^{2+} contributes to the effect of GDX on contraction in the setting of aging.

We compared the levels of major proteins involved in Ca^{2+} sequestration and efflux in ventricles from sham and GDX mice to identify the cellular mechanisms involved. Our results showed that although NCX and SERCA2 protein levels were similar in the two groups, the levels of PLB protein were dramatically higher in hearts from aging GDX mice. These observations suggest that GDX prolongs Ca^{2+} transient decay, at least in part, by increasing levels of PLB, which may reduce the rate of Ca^{2+} sequestration into the sarcoplasmic reticulum. Earlier studies of PLB protein in hearts from young adult rats and mice have consistently reported no change in PLB protein levels after GDX (9, 47, 54, 57, 62). Thus, the increase in PLB protein reported here likely reflects the combined impact of chronic testosterone deficiency and aging on the heart.

Although GDX clearly affects contractile function at the level of the ventricular myocyte, few studies have examined its effects on ventricular function in vivo. M-mode echocardiography studies have suggested that GDX reduces ejection fraction in young adult rodents (54, 60), although whether GDX affects diastolic function was not explored. Our work in aging sham and GDX mice showed that measures of systolic func-

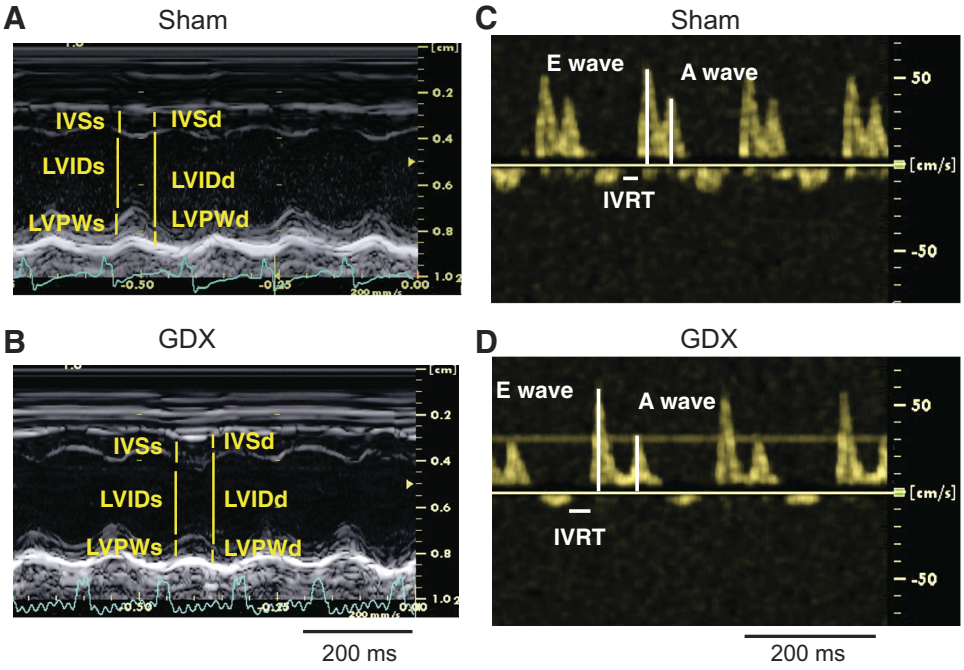

Fig. 7. Representative M-mode and Doppler echocardiography images recorded in hearts from aging sham-operated (sham) and gonadectomized (GDX) mice. *A* and *B*: representative M-mode echocardiograms of the left ventricle from aging sham and GDX mice. *C* and *D*: representative pulse-wave Doppler echocardiograms recorded from sham and GDX mice. IVSd and IVSs, interventricular septum thickness at diastole and end systole; LVIDd and LVIDs, left ventricular internal dimension at diastole and end systole; LVPWd and LVPWs, left ventricular posterior wall thickness at diastole and end systole; IVRT, isovolumic relaxation time; E wave, peak velocity of early diastolic transmitral flow; A wave, peak velocity of late transmitral flow.

tion, including ejection fraction and fractional shortening, were similar in the two groups. In contrast, pulse-wave Doppler echocardiography studies showed that long-term GDX was associated with a marked increase in isovolumic relaxation time, with no effect on *E*-to-*A* ratios or E-wave deceleration times, in the aging heart. Isovolumic relaxation time is a more reliable indicator of diastolic dysfunction in mice than either *E*-to-*A* ratios or E-wave deceleration times because of fusion of E and A waves at the rapid heart rates characteristic of mice (53). This pattern of increased isovolumic relaxation time with no change in *E*-to-*A* ratios is associated with the first stage of diastolic dysfunction (39). Our results show diastolic dysfunction with normal systolic function in aging GDX mice. This suggests that aging male GDX mice are developing HFpEF, a form of heart failure that is increasingly common in our aging population (58). However, we found no significant increase in

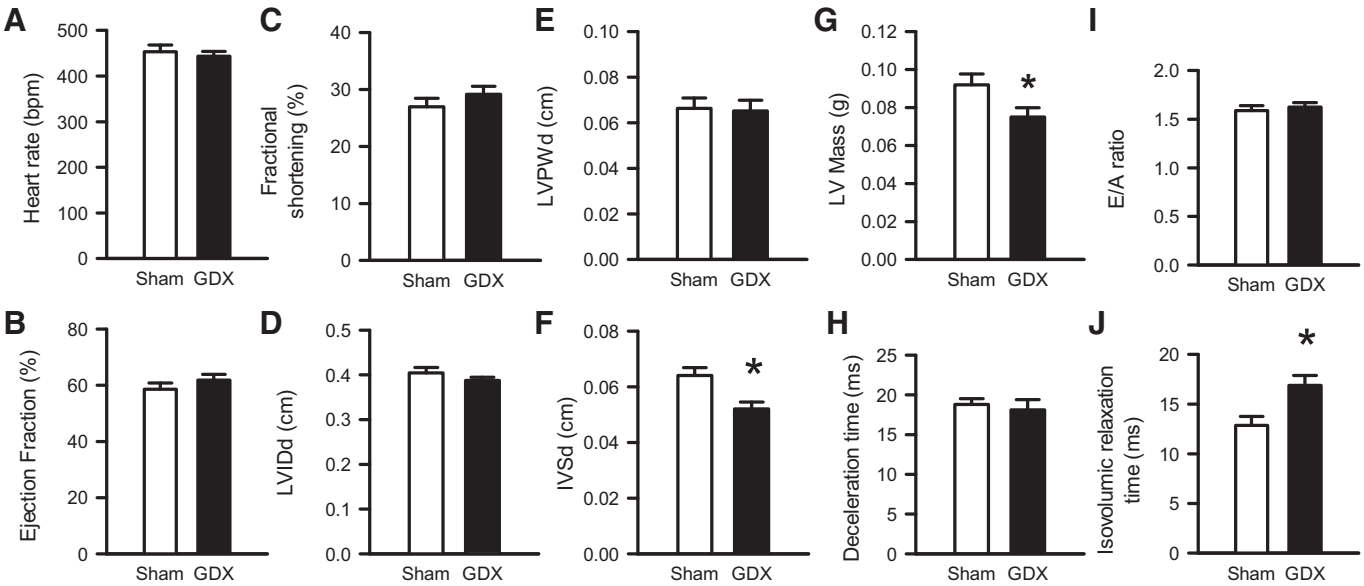

Fig. 8. Long-term gonadectomy (GDX)-induced structural and functional changes in the heart in vivo. *A–C*: M-mode echocardiography revealed that heart rate (in beats/min), ejection fraction, and fractional shortening were similar in sham-operated (sham) and GDX mice. *D–F*: the structural parameters of left ventricular internal diameter at diastole (LVIDd) and left ventricular posterior wall thickness at diastole (LVPWd) were not affected by GDX, although interventricular septum thickness at diastole (IVSd) was less in GDX than sham control mice. Similar results were observed for these parameters at systole (see Table 3). *G*: left ventricular (LV) mass was reduced in GDX mice compared with sham control mice when assessed in vivo with M-mode echocardiography. *H* and *I*: Doppler echocardiography recordings demonstrated that deceleration time and *E*-to-*A* ratio were similar in sham and GDX mice. *J*: isovolumic relaxation time was slower in aging GDX than sham mice. Values are means ± SE; $n = 22$ sham and 29 GDX mice (M-mode recordings) and 14 sham and 17 GDX mice (Doppler recordings). *$P < 0.05$ (by *t*-test).

Table 3. *Additional in vivo M-mode and pulse-wave Doppler echocardiography data from sham and GDX mice*

Parameter	Sham	GDX	*P* Value
M-mode echocardiography			
LVIDs, mm	2.99 ± 0.13 (22)	2.75 ± 0.09 (29)	0.12
LVPWs, mm	0.98 ± 0.07 (22)	0.91 ± 0.06 (29)	0.47
IVSs, mm	0.97 ± 0.04 (22)	0.86 ± 0.04 (29)	0.04*
Relative wall thickness	0.33 ± 0.03 (22)	0.31 ± 0.02 (29)	0.48
Stroke volume, ml	0.10 ± 0.01 (22)	0.09 ± 0.01 (29)	0.54
Pulse-wave Doppler echocardiography			
E wave, m/s	0.62 ± 0.02 (14)	0.57 ± 0.02 (17)	0.08
A wave, m/s	0.40 ± 0.02 (14)	0.36 ± 0.01 (17)	0.07

Values are means ± SE; sample sizes are shown in parentheses. GDX, gonadectomized; LVIDs, left ventricular internal dimension at end systole; LVPWs, left ventricular posterior wall thickness at end systole; IVSs, interventricular septum thickness at end systole; E wave, peak velocity of early diastolic transmitral flow; A wave, peak velocity of late transmitral flow. *$P < 0.05$.

lung weight in GDX mice, which suggests that they did not yet have pulmonary congestion. These findings support the further exploration of links between testosterone and HFpEF in older adults. Studies with additional markers of heart failure would also be of interest.

A novel observation reported here is that the myofilaments themselves are influenced by long-term GDX in the aging heart. Although chronic testosterone deficiency had no effect on normalized myofilament Ca^{2+} sensitivity, it did increase maximal actomyosin Mg^{2+}-ATPase activity at ~100 μM Ca^{2+}. Still, these saturating Ca^{2+} levels are much higher than physiological, so the functional significance of this finding is unclear. On the other hand, long-term GDX led to a marked decrease in phosphorylation of ELC in the aging heart. While phosphorylation of regulatory myosin light chain/myosin light chain 2 by myosin light chain kinase is well known to increase contractility, much less is known about the role of ELC and its phosphorylation in the regulation of cardiac contraction (18). It has been previously reported that ELC may affect myosin heavy chain kinetics in a manner that depends on the isoform of myosin heavy chain expression (59). These functional effects are unlikely to be a factor here, because previous studies have shown that GDX did not affect myosin heavy chain expression in the hearts of male mice (44). A recent study by Sheid and colleagues (51) examined zebrafish hearts expressing COOH-terminal ELC that is missing the S195 phosphorylation site. This de facto hypophosphorylation model produced hearts that were inefficient in their force-generating properties and rendered the zebrafish more susceptible to physical stress. Here, we found no changes in myofilament actomyosin Mg^{2+}-ATPase activity within the physiological range of Ca^{2+}, but we are unable to say if the kinetics or force-generating capacity of the myofilaments is affected. The finding by Scheid et al. (51) that the loss of a key phosphorylation site within ELC renders zebrafish hearts vulnerable to stress-induced dysfunction, combined with our novel finding that aged GDX mice have lower levels of ELC phosphorylation, may explain the increased risk for heart failure with aging in the presence of low testosterone.

Our observation that chronic testosterone deficiency slows relaxation and facilitates development of diastolic dysfunction in the aging heart is potentially important. Diastolic dysfunction and ensuing HFpEF are common in older individuals (58). The incidence of this condition is also increasing dramatically with the aging of the population, but our understanding of the pathophysiology of diastolic dysfunction is incomplete (58). To our knowledge, a role for testosterone in the pathogenesis of diastolic dysfunction has not been shown previously. Several clinical studies have suggested that low testosterone is associated with diastolic dysfunction, at least in men with cardiovascular risk factors (11, 12, 32, 56). Additional studies to explore links between testosterone deficiency, aging, and diastolic dysfunction would be of interest.

The present study also found that APD was prolonged in ventricular myocytes from aging GDX mice compared with sham-operated control mice and that this increase in APD did not account for the slower Ca^{2+} transients observed in GDX cells. Earlier studies of younger rats and mice subjected to GDX have also reported an increase in APD in both multicellular heart muscle preparations and ventricular myocytes (8, 14). This increase in APD is not due to changes in L-type Ca^{2+} current (45) but has been attributed to a reduction in the magnitude of the ultrarapid delayed rectifier K^+ current, at least in hearts from GDX mice (7). Our data suggest that this increase in APD after GDX persists in the aging heart. This may facilitate development of arrhythmias, which are common in aging men with low testosterone (5). In support of this, we did observe an increase in spontaneous contractions in ventricular myocytes isolated from GDX hearts. Additional studies with in vitro and in vivo electrophysiological recordings are required to explore this relationship further.

We also found that GDX led to a modest, but significant, decrease in ventricular myocyte size and left ventricular mass and thinner intraventricular septum compared with sham control mice. This reduction in heart size has not been reported in studies of younger mice subjected to GDX (47, 54, 62). However, these latter studies used heart weight normalized to tibia length and/or body weight to evaluate the impact of GDX on the size of the heart (47, 54, 62). We also saw no effect of GDX on heart weight when normalized to body weight or tibia length. This suggests that the effects of GDX on heart and myocyte size cannot be detected by simply weighing the tissue and that more detailed experimental approaches are needed.

The results of this study highlight a number of interesting directions for future research. Although we compared levels of Ca^{2+}-handling proteins in hearts from aging sham and GDX mice, we did not explore all relevant Ca^{2+}-handling proteins and we did not examine phosphorylation of these proteins by either protein kinase A or Ca^{2+}/calmodulin-dependent kinase II. Future experiments to investigate these pathways and their effects on phosphorylation of Ca^{2+}-handling proteins, in particular PLB, would be informative. Our study used myocytes that were paced at 2 Hz (or, in some cases, 4 Hz), which is below the physiological pacing rates seen in our echocardiography studies. It is possible that diastolic dysfunction would be exacerbated at higher pacing frequencies; additional studies at higher pacing rates would be of interest. We also found a marked decrease in circulating testosterone levels after GDX in both adult and aged mice. Testosterone also declined, but not significantly, with age in sham mice. However, we compared 5- to 6-mo-old mice with 18-mo-old mice. We might have observed an age-dependent decline in testosterone if we had used even younger sham mice and compared them with even older sham mice. Here, we subjected

mice to GDX early in life, which resulted in a model of long-term testosterone deficiency in aging mice. Similar models of early ovariectomy have been used in female mice to investigate effects of long-term estrogen deprivation (20, 35, 41, 42). In the present study, this model did allow us to detect important effects of GDX on the hearts of aging animals. However, studies in mice subjected to GDX in midlife and investigated in late life would likely be more physiologically relevant. Ultimately, it will be important to investigate whether testosterone replacement reverses the adverse effects of GDX on the aging heart. Based on the results presented here, further investigations in such a model are warranted.

In summary, long-term GDX slowed relaxation of contraction in the aging male heart. These effects were observed at the cellular level and in vivo by echocardiography. Slower contractions in ventricular myocytes from GDX mice were mediated by slower decay of the underlying Ca^{2+} transients. Additional mechanistic studies demonstrated that increased levels of PLB protein, along with hypophosphorylation of ELC, a key myofilament protein, are involved in these effects of GDX on the aging heart. Our findings indicate that testosterone deficiency causes intracellular Ca^{2+} dysregulation and myofilament dysfunction, which may facilitate development of diastolic dysfunction in aging hearts and increase the risk of heart failure.

ACKNOWLEDGMENTS

The authors are grateful to Dr. J. Q. Zhu, Elise Bisset, and Peter Nicholl for excellent technical assistance.

GRANTS

This work was supported by Canadian Institutes for Health Research Grants MOP 97973 and PGT 155961 (to S. E. Howlett) and Natural Sciences and Engineering Research Council Discovery Grant RGPIN-2018-04732 (to W. G. Pyle).

DISCLOSURES

No conflicts of interest, financial or otherwise, are declared by the authors.

AUTHOR CONTRIBUTIONS

O.A. and S.E.H. conceived and designed research; O.A., S.B., S.H.M., and W.G.P. performed experiments; O.A., S.B., S.H.-M., R.A.R., W.G.P., and S.E.H. analyzed data; O.A., S.B., S.H.-M., R.A.R., W.G.P., and S.E.H. interpreted results of experiments; O.A., W.G.P., and S.E.H. prepared figures; S.E.H. drafted manuscript; O.A., S.B., S.H.-M., R.A.R., W.G.P., and S.E.H. edited and revised manuscript; O.A., S.B., S.H.-M., R.A.R., W.G.P., and S.E.H. approved final version of manuscript.

REFERENCES

1. **Aboumsallem JP, Mishra M, Amin R, Muthuramu I, Kempen H, De Geest B.** Successful treatment of established heart failure in mice with recombinant HDL (Milano). *Br J Pharmacol* 175: 4167–4182, 2018. doi:10.1111/bph.14463.
2. **Antoons G, Mubagwa K, Nevelsteen I, Sipido KR.** Mechanisms underlying the frequency dependence of contraction and $[Ca^{2+}]_i$ transients in mouse ventricular myocytes. *J Physiol* 543: 889–898, 2002. doi:10.1113/jphysiol.2002.025619.
3. **Araujo AB, Dixon JM, Suarez EA, Murad MH, Guey LT, Wittert GA.** Endogenous testosterone and mortality in men: a systematic review and meta-analysis. *J Clin Endocrinol Metab* 96: 3007–3019, 2011. doi:10.1210/jc.2011-1137.
4. **Ayaz O, Howlett SE.** Testosterone modulates cardiac contraction and calcium homeostasis: cellular and molecular mechanisms. *Biol Sex Differ* 6: 9, 2015. doi:10.1186/s13293-015-0027-9.
5. **Bell JR, Bernasochi GB, Varma U, Raaijmakers AJ, Delbridge LM.** Sex and sex hormones in cardiac stress—mechanistic insights. *J Steroid Biochem Mol Biol* 137: 124–135, 2013. doi:10.1016/j.jsbmb.2013.05.015.
6. **Blenck CL, Harvey PA, Reckelhoff JF, Leinwand LA.** The importance of biological sex and estrogen in rodent models of cardiovascular health and disease. *Circ Res* 118: 1294–1312, 2016. doi:10.1161/CIRCRESAHA.116.307509.
7. **Brouillette J, Trépanier-Boulay V, Fiset C.** Effect of androgen deficiency on mouse ventricular repolarization. *J Physiol* 546: 403–413, 2003. doi:10.1113/jphysiol.2002.030460.
8. **Brouillette J, Rivard K, Lizotte E, Fiset C.** Sex and strain differences in adult mouse cardiac repolarization: importance of androgens. *Cardiovasc Res* 65: 148–157, 2005. doi:10.1016/j.cardiores.2004.09.012.
9. **Callies F, Strömer H, Schwinger RH, Bölck B, Hu K, Frantz S, Leupold A, Beer S, Allolio B, Bonz AW.** Administration of testosterone is associated with a reduced susceptibility to myocardial ischemia. *Endocrinology* 144: 4478–4483, 2003. doi:10.1210/en.2003-0058.
10. **Corona G, Rastrelli G, Monami M, Guay A, Buvat J, Sforza A, Forti G, Mannucci E, Maggi M.** Hypogonadism as a risk factor for cardiovascular mortality in men: a meta-analytic study. *Eur J Endocrinol* 165: 687–701, 2011. doi:10.1530/EJE-11-0447.
11. **Čulić V, Bušić Ž.** Testosterone may influence left ventricular diastolic function depending on previous myocardial infarction and smoking. *Int J Cardiol* 186: 67–71, 2015. doi:10.1016/j.ijcard.2015.03.238.
12. **Čulić V.** Testosterone and cardiac diastolic function. *J Am Coll Cardiol* 68: 573–574, 2016. doi:10.1016/j.jacc.2016.03.604.
13. **Curl CL, Delbridge LM, Canny BJ, Wendt IR.** Testosterone modulates cardiomyocyte Ca^{2+} handling and contractile function. *Physiol Res* 58: 293–297, 2009.
14. **D'Antona G, Gualea MR, Ceriani T.** Effects of gonadectomy, testosterone replacement and supplementation on cardiac action potentials in the rat. *Basic Appl Myol* 11: 23–29, 2001.
15. **Dart DA, Waxman J, Aboagye EO, Bevan CL.** Visualising androgen receptor activity in male and female mice. *PLoS One* 8: e71694, 2013. doi:10.1371/journal.pone.0071694.
16. **Davey RA, Grossmann M.** Androgen receptor structure, function and biology: from bench to bedside. *Clin Biochem Rev* 37: 3–15, 2016.
17. **Eleawa SM, Sakr HF, Hussein AM, Assiri AS, Bayoumy NM, Alkhateeb M.** Effect of testosterone replacement therapy on cardiac performance and oxidative stress in orchidectomized rats. *Acta Physiol (Oxf)* 209: 136–147, 2013. doi:10.1111/apha.12158.
18. **England J, Loughna S.** Heavy and light roles: myosin in the morphogenesis of the heart. *Cell Mol Life Sci* 70: 1221–1239, 2013. doi:10.1007/s00018-012-1131-1.
19. **Fares E, Howlett SE.** Effect of age on cardiac excitation-contraction coupling. *Clin Exp Pharmacol Physiol* 37: 1–7, 2010. doi:10.1111/j.1440-1681.2009.05276.x.
20. **Fares E, Parks RJ, Macdonald JK, Egar JMS, Howlett SE.** Ovariectomy enhances SR Ca^{2+} release and increases Ca^{2+} spark amplitudes in isolated ventricular myocytes. *J Mol Cell Cardiol* 52: 32–42, 2012. doi:10.1016/j.yjmcc.2011.09.002.
21. **Ferrier GR, Redondo IM, Mason CA, Mapplebeck C, Howlett SE.** Regulation of contraction and relaxation by membrane potential in cardiac ventricular myocytes. *Am J Physiol Heart Circ Physiol* 278: H1618–H1626, 2000. doi:10.1152/ajpheart.2000.278.5.H1618.
22. **Feridooni HA, Dibb KM, Howlett SE.** How cardiomyocyte excitation, calcium release and contraction become altered with age. *J Mol Cell Cardiol* 83: 62–72, 2015. doi:10.1016/j.yjmcc.2014.12.004.
23. **Feridooni HA, Kane AE, Ayaz O, Boroumandi A, Polidovitch N, Tsushima RG, Rose RA, Howlett SE.** The impact of age and frailty on ventricular structure and function in C57BL/6J mice. *J Physiol* 595: 3721–3742, 2017. doi:10.1113/JP274134.
24. **Feridooni HA, MacDonald JK, Ghimire A, Pyle WG, Howlett SE.** Acute exposure to progesterone attenuates cardiac contraction by modifying myofilament calcium sensitivity in the female mouse heart. *Am J Physiol Heart Circ Physiol* 312: H46–H59, 2017. doi:10.1152/ajpheart.00073.2016.
25. **Gencer B, Mach F.** Testosterone: a hormone preventing cardiovascular disease or a therapy increasing cardiovascular events? *Eur Heart J* 37: 3569–3575, 2016. doi:10.1093/eurheartj/ehv439.
26. **Ghimire A, Kane AE, Howlett SE.** Sex differences in the physiology and pathology of the aging heart. In: *The Encyclopedia of Cardiovascular Research and Medicine*, edited by Vasan R, Sawyer D. Oxford: Elsevier, 2018, vol. 4, p. 368–376.

27. **Golden KL, Marsh JD, Jiang Y, Brown T, Moulden J.** Gonadectomy of adult male rats reduces contractility of isolated cardiac myocytes. *Am J Physiol Endocrinol Metab* 285: E449–E453, 2003. doi:10.1152/ajpendo.00054.2003.
28. **Grandy SA, Howlett SE.** Cardiac excitation-contraction coupling is altered in myocytes from aged male mice but not in cells from aged female mice. *Am J Physiol Heart Circ Physiol* 291: H2362–H2370, 2006. doi:10.1152/ajpheart.00070.2006.
29. **Güder G, Frantz S, Bauersachs J, Allolio B, Ertl G, Angermann CE, Störk S.** Low circulating androgens and mortality risk in heart failure. *Heart* 96: 504–509, 2010. doi:10.1136/hrt.2009.181065.
30. **Howlett SE.** Age-associated changes in excitation-contraction coupling are more prominent in ventricular myocytes from male rats than in myocytes from female rats. *Am J Physiol Heart Circ Physiol* 298: H659–H670, 2010. doi:10.1152/ajpheart.00214.2009.
31. **Jankowska EA, Biel B, Majda J, Szklarska A, Lopuszanska M, Medras M, Anker SD, Banasiak W, Poole-Wilson PA, Ponikowski P.** Anabolic deficiency in men with chronic heart failure: prevalence and detrimental impact on survival. *Circulation* 114: 1829–1837, 2006. doi:10.1161/CIRCULATIONAHA.106.649426.
32. **Jin Q, Lou Y, Chen H, Li T, Bao X, Liu Q, He X.** Lower free testosterone level is correlated with left ventricular diastolic dysfunction in asymptomatic middle-aged men with type 2 diabetes mellitus. *Int J Clin Pract* 68: 1454–1461, 2014. doi:10.1111/ijcp.12481.
33. **Keller KM, Howlett SE.** Sex differences in the biology and pathology of the aging heart. *Can J Cardiol* 32: 1065–1073, 2016. doi:10.1016/j.cjca.2016.03.017.
34. **Kloner RA, Carson C III, Dobs A, Kopecky S, Mohler ER III.** Testosterone and cardiovascular disease. *J Am Coll Cardiol* 67: 545–557, 2016. doi:10.1016/j.jacc.2015.12.005.
35. **Lizotte E, Grandy SA, Tremblay A, Allen BG, Fiset C.** Expression, distribution and regulation of sex steroid hormone receptors in mouse heart. *Cell Physiol Biochem* 23: 75–86, 2009. doi:10.1159/000204096.
36. **Marsh JD, Lehmann MH, Ritchie RH, Gwathmey JK, Green GE, Schiebinger RJ.** Androgen receptors mediate hypertrophy in cardiac myocytes. *Circulation* 98: 256–261, 1998. doi:10.1161/01.CIR.98.3.256.
37. **Menazza S, Murphy E.** The expanding complexity of estrogen receptor signaling in the cardiovascular system. *Circ Res* 118: 994–1007, 2016. doi:10.1161/CIRCRESAHA.115.305376.
38. **Mozaffarian D, Benjamin EJ, Go AS, Arnett DK, Blaha MJ, Cushman M, Das SR, de Ferranti S, Després JP, Fullerton HJ, Howard VJ, Huffman MD, Isasi CR, Jiménez MC, Judd SE, Kissela BM, Lichtman JH, Lisabeth LD, Liu S, Mackey RH, Magid DJ, McGuire DK, Mohler ER III, Moy CS, Muntner P, Mussolino ME, Nasir K, Neumar RW, Nichol G, Palaniappan L, Pandey DK, Reeves MJ, Rodriguez CJ, Rosamond W, Sorlie PD, Stein J, Towfighi A, Turan TN, Virani SS, Woo D, Yeh RW, Turner MB; Writing Group Members; American Heart Association Statistics Committee; Stroke Statistics Subcommittee.** Heart disease and stroke statistics—2016 update: a report from the American Heart Association. *Circulation* 133: e38–e360, 2016. [Erratum in *Circulation* 133: e599, 2016.] doi:10.1161/CIR.0000000000000350.
39. **Nagueh SF, Appleton CP, Gillebert TC, Marino PN, Oh JK, Smiseth OA, Waggoner AD, Flachskampf FA, Pellikka PA, Evangelisa A.** Recommendations for the evaluation of left ventricular diastolic function by echocardiography. *Eur J Echocardiogr* 10: 165–193, 2009. doi:10.1093/ejechocard/jep007.
40. **Oskui PM, French WJ, Herring MJ, Mayeda GS, Burstein S, Kloner RA.** Testosterone and the cardiovascular system: a comprehensive review of the clinical literature. *J Am Heart Assoc* 2: e000272, 2013. doi:10.1161/JAHA.113.000272.
41. **Parks RJ, Ray G, Bienvenu LA, Rose RA, Howlett SE.** Sex differences in SR Ca^{2+} release in murine ventricular myocytes are regulated by the cAMP/PKA pathway. *J Mol Cell Cardiol* 75: 162–173, 2014. doi:10.1016/j.yjmcc.2014.07.006.
42. **Parks RJ, Bogachev O, Mackasey M, Ray G, Rose RA, Howlett SE.** The impact of ovariectomy on cardiac excitation-contraction coupling is mediated through cAMP/PKA-dependent mechanisms. *J Mol Cell Cardiol* 111: 51–60, 2017. doi:10.1016/j.yjmcc.2017.07.118.
43. **Pastor-Pérez FJ, Manzano-Fernández S, Garrido Bravo IP, Nicolás F, Tornel PL, Lax A, de la Morena G, Valdés M, Pascual-Figal DA.** Anabolic status and functional impairment in men with mild chronic heart failure. *Am J Cardiol* 108: 862–866, 2011. doi:10.1016/j.amjcard.2011.05.016.
44. **Patrizio M, Musumeci M, Piccone A, Raggi C, Mattei E, Marano G.** Hormonal regulation of β-myosin heavy chain expression in the mouse left ventricle. *J Endocrinol* 216: 287–296, 2013. doi:10.1530/JOE-12-0201.
45. **Pham TV, Robinson RB, Danilo P Jr, Rosen MR.** Effects of gonadal steroids on gender-related differences in transmural dispersion of L-type calcium current. *Cardiovasc Res* 53: 752–762, 2002. doi:10.1016/S0008-6363(01)00449-7.
46. **Regitz-Zagrosek V, Kararigas G.** Mechanistic pathways of sex differences in cardiovascular disease. *Physiol Rev* 97: 1–37, 2017. doi:10.1152/physrev.00021.2015.
47. **Ribeiro Júnior RF, Ronconi KS, Jesus ICG, Almeida PWM, Forechi L, Vassallo DV, Guatimosim S, Stefanon I, Fernandes AA.** Testosterone deficiency prevents left ventricular contractility dysfunction after myocardial infarction. *Mol Cell Endocrinol* 460: 14–23, 2018. doi:10.1016/j.mce.2017.06.011.
48. **Rosano GM, Spoletini I, Vitale C.** Cardiovascular disease in women, is it different to men? The role of sex hormones. *Climacteric* 20: 125–128, 2017. [Erratum in *Climacteric* 21: 92, 2018.] doi:10.1080/13697137.2017.1291780.
49. **Ruige JB, Mahmoud AM, De Bacquer D, Kaufman JM.** Endogenous testosterone and cardiovascular disease in healthy men: a meta-analysis. *Heart* 97: 870–875, 2011. doi:10.1136/hrt.2010.210757.
50. **Schaible TF, Malhotra A, Ciambrone G, Scheuer J.** The effects of gonadectomy on left ventricular function and cardiac contractile proteins in male and female rats. *Circ Res* 54: 38–49, 1984. doi:10.1161/01.RES.54.1.38.
51. **Scheid LM, Mosqueira M, Hein S, Kossack M, Juergensen L, Mueller M, Meder B, Fink RH, Katus HA, Hassel D.** Essential light chain S195 phosphorylation is required for cardiac adaptation under physical stress. *Cardiovasc Res* 111: 44–55, 2016. doi:10.1093/cvr/cvw066.
52. **Scheuer J, Malhotra A, Schaible TF, Capasso J.** Effects of gonadectomy and hormonal replacement on rat hearts. *Circ Res* 61: 12–19, 1987. doi:10.1161/01.RES.61.1.12.
53. **Schnelle M, Catibog N, Zhang M, Nabeebaccus AA, Anderson G, Richards DA, Sawyer G, Zhang X, Toischer K, Hasenfuss G, Monaghan MJ, Shah AM.** Echocardiographic evaluation of diastolic function in mouse models of heart disease. *J Mol Cell Cardiol* 114: 20–28, 2018. doi:10.1016/j.yjmcc.2017.10.006.
54. **Sebag IA, Gillis MA, Calderone A, Kasneci A, Meilleur M, Haddad R, Noiles W, Patel B, Chalifour LE.** Sex hormone control of left ventricular structure/function: mechanistic insights using echocardiography, expression, and DNA methylation analyses in adult mice. *Am J Physiol Heart Circ Physiol* 301: H1706–H1715, 2011. doi:10.1152/ajpheart.00088.2011.
55. **Shutt RH, Howlett SE.** Hypothermia increases the gain of excitation-contraction coupling in guinea pig ventricular myocytes. *Am J Physiol Cell Physiol* 295: C692–C700, 2008. doi:10.1152/ajpcell.00287.2008.
56. **Tinetti M, Gysel M, Farias J, Ferrer M, Lombardero M, Baranchuk A.** Left ventricular filling pressure in male patients with type 2 diabetes and normal versus low total testosterone levels. *Cardiol J* 22: 206–211, 2015. doi:10.5603/CJ.a2014.0056.
57. **Tsang S, Wong SS, Wu S, Kravtsov GM, Wong TM.** Testosterone-augmented contractile responses to α_1- and β_1-adrenoceptor stimulation are associated with increased activities of RyR, SERCA, and NCX in the heart. *Am J Physiol Cell Physiol* 296: C766–C782, 2009. doi:10.1152/ajpcell.00193.2008.
58. **Upadhya B, Kitzman DW.** Heart failure with preserved ejection fraction in older adults. *Heart Fail Clin* 13: 485–502, 2017. doi:10.1016/j.hfc.2017.02.005.
59. **Wang Y, Ajtai K, Kazmierczak K, Szczesna-Cordary D, Burghardt TP.** N-terminus of cardiac myosin essential light chain modulates myosin step-size. *Biochemistry* 55: 186–198, 2016. doi:10.1021/acs.biochem.5b00817.
60. **Weerateerangkul P, Shinlapawittayatorn K, Palee S, Apaijai N, Chattipakorn SC, Chattipakorn N.** Early testosterone replacement attenuates intracellular calcium dyshomeostasis in the heart of testosterone-deprived male rats. *Cell Calcium* 67: 22–30, 2017. doi:10.1016/j.ceca.2017.08.003.
61. **Wehr E, Pilz S, Boehm BO, März W, Grammer T, Obermayer-Pietsch B.** Low free testosterone is associated with heart failure mortality in older men referred for coronary angiography. *Eur J Heart Fail* 13: 482–488, 2011. doi:10.1093/eurjhf/hfr007.
62. **Witayavanitkul N, Woranush W, Bupha-Intr T, Wattanapermpool J.** Testosterone regulates cardiac contractile activation by modulating

SERCA but not NCX activity. *Am J Physiol Heart Circ Physiol* 304: H465–H472, 2013. doi:10.1152/ajpheart.00555.2012.

63. **Yang FH, Pyle WG.** Reduced cardiac CapZ protein protects hearts against acute ischemia-reperfusion injury and enhances preconditioning. *J Mol Cell Cardiol* 52: 761–772, 2012. doi:10.1016/j.yjmcc.2011.11.013.
64. **Yeap BB, Flicker L.** Hormones and cardiovascular disease in older men. *J Am Med Dir Assoc* 15: 326–333, 2014. doi:10.1016/j.jamda.2013.12.004.
65. **Yeap BB.** Testosterone and cardiovascular disease risk. *Curr Opin Endocrinol Diabetes Obes* 22: 193–202, 2015. doi:10.1097/MED.0000000000000161.